HHS Public Access

Author manuscript

Circ Arrhythm Electrophysiol. Author manuscript; available in PMC 2019 June 01.

Published in final edited form as:

Circ Arrhythm Electrophysiol. 2018 June ; 11(6): e005414. doi:10.1161/CIRCEP.117.005414.

Transient Outward K+ Current (I_{to}) Underlies the Right Ventricular Initiation of Polymorphic Ventricular Tachycardia in a Transgenic Rabbit Model of Long QT Type 1

Bum-Rak Choi, PhD[1], **Weiyan Li, PhD**[1], **Dmitry Terentyev, PhD**[1], **Anatoli Y. Kabakov, PhD**[1], **Mingwang Zhong, BS**[2], **Colin M Rees, PhD**[2], **Radmila Terentyeva, MS**[1], **Tae Yun Kim, PhD**[1], **Zhilin Qu, PhD**[4], **Xuwen Peng, DVM, MD**[3], **Alain Karma, PhD**[2], and **Gideon Koren, MD**[1]

[1]Cardiovascular Research Center, Division of Cardiology, Rhode Island Hospital, Warren Alpert Medical School of Brown University, Providence, RI

[2]Department of Physics, Northeastern University, Boston MA

[3]Department of Comparative Medicine, Pennsylvania State University College of Medicine, Hershey, PA

[4]Department of Medicine (Cardiology), University of California, Los Angeles, CA

Abstract

Background—Sudden death in long QT syndrome type 1 (LQT1), an inherited disease caused by loss-of-function mutations in KCNQ1, is triggered by early afterdepolarizations (EADs) that initiate polymorphic VT (pVT). We investigated ionic mechanisms that underlie pVT in LQT1 using a transgenic rabbit model of LQT1.

Methods and Results—Optical mapping, cellular patch clamping, and computer modeling were used to elucidate the mechanisms of EADs in transgenic LQT1 rabbits. The results showed that shorter APD in the right ventricle (RV) was associated with focal activity during pVT initiation. RV cardiomyocytes demonstrated higher incidence of EADs under 50 nM isoproterenol. Voltage-clamp studies revealed that the transient outward potassium current (I_{to}) magnitude was 28% greater in RV associated with KChiP2 but with no differences in terms of calcium-cycling kinetics and other sarcolemmal currents. Perfusing with the I_{to} blocker 4-aminopyridine changed the initial focal sites of pVT from the RV to the LV, corroborating the role of I_{to} in pVT initiation. Computer modeling showed that EADs occur preferentially in the RV due to the larger conductance of the slow inactivating component of I_{to}, which repolarizes the membrane potential sufficiently rapidly to allow reactivation of $I_{Ca,L}$ before I_{Kr} has had sufficient time to activate.

Conclusions—I_{to} heterogeneity creates both triggers and an arrhythmogenic substrate in LQT1. In the absence of I_{Ks}, I_{to} interactions with $I_{Ca,L}$ and I_{Kr} promote EADs in the RV while prolonging

Correspondence: Bum-Rak Choi, PhD, Cardiovascular Research Center, Rhode Island Hospital &, Brown Medical School, Providence, RI 02903, Tel: (401) 444-6129, Fax: (401) 444-9203, Bum-Rak_Choi@brown.edu. Gideon Koren, MD, Cardiovascular Research Center, Rhode Island Hospital & School, Brown Medical School, Providence, RI 02903, Tel: (401) 444-6129, Fax: (401) 444-9203, Gideon_Koren@brown.edu.

Disclosures: none

APD in the LV. This heterogeneity of action potential enhances dispersion of refractoriness and facilitates conduction blocks that initiate pVTs.

Keywords

long QT syndrome; action potential; ventricular tachycardia; early afterdepolarization; transient outward potassium current; APD dispersion

Journal Subject Terms

Arrhythmias; Electrophysiology; Mechanisms; Basic Science Research

Introduction

Long-QT syndrome type 1 (LQT1) is an inherited disease associated with prolongation of QT intervals in ECG recordings and an increased risk for developing polymorphic ventricular tachycardia (pVT) that underlies syncope and SCD.[1] The disease is caused by loss-of-function mutations in the KCNQ1 gene, which encodes the pore-forming α subunit of the slowly activating delayed rectifier repolarizing K^+ current (I_{Ks}). LQT1 is the most common form of long QT syndrome and accounts for almost half of genotyped cases.[2] Arrhythmias and SCD in LQT1 are often precipitated by prolonged periods of exercise that sustains sympathetic activity and can in turn trigger early afterdepolarizations (EADs) that initiate pVTs.[3]

Experimental models using I_{Ks} blockers such as chromanol or HMR1556 to mimic LQT1 have been helpful in elucidating the roles of I_{Ks} in APD dynamics.[4, 5] While chromanol perfusion produces limited APD prolongation, persistent sympathetic stimulation can both prolong APD significantly and enhance APD dispersion.[5] Clinical data have also demonstrated that the $T_{peak} - T_{end}$ intervals of surface ECGs were accentuated during exercise tests only in LQT1 patients but not in LQT2 patients,[6] supporting the notion that APD dispersion plays significant roles in pVT initiation in LQT1. Although experimental models with chromanol demonstrated enhanced APD dispersion, chromanol often failed to induce EADs.[7] In addition, non-specific action of chromanol such as blocking transient outward K^+ current (I_{to})[8] limits the translation of these findings from the experimental models to congenital LQT1-related arrhythmias.

We have generated a transgenic rabbit model for LQT1 syndrome by overexpressing a pore mutant of KCNQ1 (KCNQ1-Y315S) in the heart.[9] Our previous studies of LQT1 rabbits show that LQT1 rabbits develop EADs and pVTs following sympathetic stimulation,[10, 11] and all LQT1 rabbits die within three weeks after slowing their heart rate with acute ablation of the AV node *in vivo*. Detailed mapping revealed that triggered activity mostly originated in the right ventricle (RV) despite shorter APD in RV compared to LV.[10] Due to the formation of triggered activity in short-APD regions, its propagation often encountered conduction blocks and promoted reentry formation in LQT1 rabbits.[10]

The present study was designed to elucidate the molecular mechanisms underlying tissue heterogeneity and EAD formation in LQT1 rabbits. Here we combine electrophysiological

studies, optical mapping, and computational modeling to delineate the mechanisms underlying paradoxical EAD formation from the RV despite shorter APD than in the LV. The present study demonstrates that the lack of I_{Ks} in LQT1 unmasks the critical role of I_{to} heterogeneity in promoting EADs preferentially in the RV by its effect on AP plateau voltage, I_{CaL} and I_{Kr}, and the initiation of arrhythmias.

Methods

The authors declare that all supporting data and computer simulation source code are available within the article and its supplementary files.

Heart Preparation

LQT1 rabbits of either sex, averaging 16.5 months old / 4.2 kg body weight / 9.14 g heart weight, were euthanized with buprenorphene (0.03 mg/kg IM), acepromazine (0.5 $mg.kg^{-1}$ IM), xylazene (15 $mg.kg^{-1}$ IM), ketamine (60 $mg.kg^{-1}$ IM), pentothal (35 $mg.kg^{-1}$ IV), and heparin (200 $U.kg^{-1}$). This investigation conformed to the current Guide for Care and Use of Laboratory Animals published by the National Institutes of Health (National Academies Press, revised 2011) and approved by the Lifespan Animal Welfare Committee at Rhode Island Hospital. Detailed methods for optical mapping are available in the supplemental material.

Patch Clamping

Isolation of cardiomyocytes by standard enzymatic techniques and patch-clamp recordings were performed as described previously.[9] RV and LV (septal region) myocytes were isolated from hearts (n=5 hearts each from LQT1 and LMC). Whole-cell recordings (11–18 cardiomyocytes per group) were obtained with an Axopatch-200B amplifier (Axon Instruments) with standard patch-clamp techniques (see supplemental material for detail). Our voltage-clamp data on I_{to} indicates that the inactivation of I_{to} is well fit by the sum of two exponentials

$$I_{to,total} = I_{to,fi} \exp(-t/\tau_{fi}) + I_{to,si} \exp(-t/\tau_{si}) \quad (1)$$

where $I_{to,total}$ is the total I_{to} current, $I_{to,fi}$ and $I_{to,si}$ are the amplitudes of the fast-inactivating (fi) and slow-inactivating (si) components, respectively. It should be emphasized that $I_{to,fi}$ and $I_{to,si}$ represent the fast and slow *inactivating* components of $I_{to,total}$ and in principle contain contributions from both $I_{to,f,}$ (Kv4.2/Kv4.3) and $I_{to,s}$ (Kv1.4) that inactivate on similar time scales,[12] but recover from inactivation on very different time scales.[13] To determine the recovery kinetics from inactivation of I_{to}, a double-pulse protocol with variable interpulse intervals ranging from 50 ms to 15 seconds was used (see supplemental material for detail). Decay of each I_{to} current evoked by each 2nd pulse was fit to a double exponential decay to determine the magnitude of the fast and slow inactivating components of the current. The amplitude of each component as a function of inter-pulse interval was fit to a double exponential recovery function to determine the magnitude of the fast and slow recovering components of each decay component.

Confocal Ca^{2+} recording

Cytosolic and intra-SR Ca^{2+} changes were monitored using a Leica TCS SP5 II confocal system in line-scan mode, and V_m were simultaneously recorded with the patch-clamp technique.[14] Ca^{2+} transients were recorded in intact cells loaded with Fluo-3-AM at 0.25 Hz field stimulation in the presence of 50 nM isoproterenol. Detailed methods for confocal Ca^{2+} imaging are available in the supplemental material.

Western blots of I_{to} and Ca^{2+}-handling proteins

Western blotting of Kv1.4, Kv4.2, Kv4.3, and KChIP2 were performed as described in [13]. Membranes from RV and LV heart (atria dissected away) were isolated by homogenization. The antibodies for Kv1.4, Kv4.2, and KChIP2 were purchased from Alomone Labs (Jerusalem, Israel). Western blot analyses of Ca^{2+}-handling proteins were performed as described in [14]. Detailed methods are available in the supplemental material.

Computer modeling of rabbit myocytes

We used the rabbit ventricular myocyte model of Mahajan et al.[15] with modified mathematical formulations of $I_{to,}$ I_{Kr}, and $I_{Ca,L}$ that quantitatively reproduce voltage-clamp data obtained from LQT1 rabbits under isoproterenol. Following the double-exponential form of Equation (1), I_{to} was modeled as the sum of $I_{to,fi}$ and $I_{to,si}$ with different conductances and kinetics in RV and LV. I_{Kr} and $I_{Ca,L}$ were taken to be the same in RV and LV consistent with experimental data. We model I_{Kr} using the multi-state Markov model of Mazhari et al.[16] with parameters fitted to our patch clamp measurements that reproduce the slow-activation kinetics of I_{Kr} in the V_m range relevant for EAD formation. In addition, we use a novel formulation of $I_{Ca,L}$ gating to quantitatively fit voltage-clamp data under isoproterenol. Details of the ionic model are provided in the supplemental material.

Statistical Analysis

Optical mapping data of intact heart are presented as means ± SD and single cell data are presented as means ± SEM. For normally distributed values, we used Student's *t*-test (paired and unpaired) to compare the means of two groups and ANOVA to compare multiple means. A 2-side p value of ≤ 0.05 was considered significant. Origin software (OriginLab, Northampton, MA) was used for Shapiro-Wilk normality test, Student's t-test, and ANOVA. Fisher's exact test was used for categorical variables using GraphPad software (San Diego, CA).

Results

Potential role of I_{to} in pVT initiation in LQT1 rabbits

Previous optical mapping study of LQT1 rabbits revealed that APD dispersion became pronounced under slow heart rate (> 1 sec) mostly due to shorter APD in RV than in LV.[10] Paradoxically, most pVTs were started from premature ventricular complex originating from RV despite shorter APD in RV.[10] We hypothesized that I_{to} plays a major role in APD gradient and pVT initiation between RV and LV. To test this hypothesis, we investigated the effect of the I_{to} blocker 4-Aminopyridine (4-AP) on arrhythmia initiation and APD gradient.

Figure 1A shows sample traces and APD maps under 0 and 0.5 mM 4-AP. Control APD in RV (red) is shorter than the LV, but 4-AP markedly prolonged APD in RV, causing inversion of the APD gradient between RV and LV (Figure 1A) while LMC hearts did not (see supplementary Figure S2). The addition of isoproterenol induced VT/VF, but the initiation of VT/VF was from the LV rather than the RV (5 out of 7 VTs originated from the LV, n=5 hearts) (Figure 1B&C). These results strongly suggest that higher I_{to} density in RV plays an important role in shortening APD in the RV and initiating EADs from that region.

RV CMs origin of EADs in LQT1 rabbits

To verify the origin of EADs at the cellular scale, we isolated single myocytes from RV and LV and investigated their propensity to generate EADs under isoproterenol. Figure 2A shows V_m recordings from RV (red) and LV (blue) myocytes (n=12 per group) under 50 nmol/L isoproterenol. In line with the intact heart optical mapping study, current-clamp experiments on single cardiomyocytes (CMs) isolated from the RV of LQT1 rabbits showed frequent EADs, while myocytes from the LV did not show EADs (Figure 2A&B). CMs from LMC rabbits did not show EADs under 50 nmol/L isoproterenol (see Supplementary Figure S3). Note that despite the prolonged APD of LV CMs, V_m at the plateau did not oscillate to form EADs (blue traces in panel A). Detailed examination of V_m traces at expanded time scale (Figure 2C) suggests that the initial plateau V_m is substantially lower than that of LV CMs. Of note, this lower plateau V_m was associated with large-amplitude EADs. EADs were not induced under the same condition in LMC CMs (supplementary Figure S3).

Previous studies indicated a general association between prolongation of APD and risk for EADs. In LQT1, APD_{90} was substantially longer in LV CMs vs. RV CMs (Figure 2D), yet EADs were more frequent in RV CMs than LV CMs. Further analysis of APD_{30}/APD_{90} (Figure 2E) show that the action potentials of RV cells have rapid repolarization during the early phase of the action potential (phase 1 period). Thus, these data show that in the case of LQT1 rabbits, EADs originate from a region (RV) with a shorter APD, both at the cellular scale and the tissue scale (reference[10] and Figure 1).

I_{to} is larger in RV CMs

Given the shape of the action potential and the rapid initial repolarization, we hypothesized that the main difference between RV and LV LQT1 CMs is I_{to}. The ionic currents were measured using voltage clamp under isoproterenol (50 nmol/L). The results show a substantially higher peak I_{to} amplitude in RV CMs than LV CMs (Figure 3A–C).

I_{to} inactivation kinetics from our voltage-clamp measurements could be best fitted with two exponential decays (see Equation (1) and Figure 3A–B). We separated these two exponential decays (see Methods for details): a fast-inactivation component marked as $I_{to,fi}$ with a time constant of τ_{fi} and a slow-inactivating component as $I_{to,si}$ with a time constant of τ_{si}. Detailed analysis of two components revealed that $I_{to,fi}$ and $I_{to,si}$ are 30% and 83% greater in RV ($g_{to,fi}$ = 0.068±0.005 mS/μF and $g_{to,si}$ = 0.033±0.005 mS/μF) than LV CMs ($g_{to,fi}$ = 0.052±0.005 mS/μF and $g_{to,si}$ = 0.018±0.002 mS/μF, see panel D), respectively. The τ_{fi} were not significantly different, but the τ_{si} of the slow component was 25% slower in RV CMs (τ_{si} = 73±6.7 ms in RV vs. 59±6.9 ms at high voltage, see panel E).

It is generally thought that I_{to} in rabbits recovers slowly from inactivation ($I_{to,s}$) and makes only a limited contribution to APD. We investigated I_{to} recovery kinetics using a double-pulse protocol (Figure 4A). We found that rabbit CMs have a substantial magnitude of $I_{to,f}$ (τ_{fast} = 19.5 ms), which was larger in RV compared to LV myocytes ($I_{to,f}$ = 8.9±1.7 and 5.3±1.6 pA/pF for RV and LV respectively, Figure 4B–C). $I_{to,s}$ (τ_{slow} = 3.41 sec) was similar in RV and LV. In addition, the recovery of $I_{to,si}$ was analyzed by separating fast- and slow-inactivation components of I_{to} during the double-pulse I_{to} recovery protocol. The slowly inactivating component of I_{to} was significantly larger in RV vs. LV (8.6±1.5 and 3.2±0.76 pA/pF for RV and LV respectively, $p < 0.05$). This results in a significant difference in the amount of available $I_{to,si}$ when the interpulse interval is >600 ms (Figure 4B).

The expression of K^+ channel interacting protein (KChIP2) was significantly higher in RV (Figure 4D–E) but the western blots of Kv4.2 and Kv1.4 of RV and LV CMs (panel D and Figure S6) were not significantly different. Since KChIP2 modulates $I_{to,f}$ channel expression and kinetics, higher KChIP2 expression in RV likely provides molecular mechanisms underlying differences of $I_{to,f}$ magnitude and kinetics between RV and LV myocytes.

Of note, there were no significant differences in $I_{Ca,L}$ or its inactivation properties as well as I_{Kr} and I_{K1} between RV and LV myocytes under 50 nmol/L isoproterenol (Figure 5A–C). These results strongly suggest that I_{to} is responsible for APD gradient and RV-specific EAD formation in LQT1 rabbits.

Ca^{2+} handling between RV and LV CMs

Ca^{2+} handling and its coupling with voltage have frequently been suspected of promoting EADs.[17] Our previous studies of EAD mechanisms in LQT2 rabbits also demonstrated that abnormal Ca^{2+} dynamics and leaky ryanodine receptors increased the forward mode of the electrogenic Na^+/Ca^{2+} exchanger (I_{NCX}), slowing down repolarization and allowing reactivation of the $I_{Ca,L}$ window current to produce EADs.[14] We therefore investigated whether differences in Ca^{2+} handling between RV and LV myocytes in LQT1 rabbits underlie preferential EAD formation in RV using confocal Ca^{2+} imaging. Figure 6 shows an example of simultaneous recordings of V_m, cytosolic and SR Ca^{2+} during action potentials. Panels A&B show typical examples of V_m and Ca^{2+} from RV and LV CMs. The amplitude and the fractional release of Ca^{2+} from SR did not differ between RV and LV myocytes. We found no significant difference in Ca^{2+} handling between RV and LV (panel C–E), suggesting that Ca^{2+} handling does not underlie preferential EAD formation in RV myocytes. Western blots of Ca^{2+}-handling proteins from RV and LV were not significantly different (see supplementary Figure S7).

I_{to} facilitates EAD formation: Computer-modeling studies

We examined whether computer modeling could reproduce the AP waveforms in RV and LV under isoproterenol, only through varying $I_{to.}$ Figure 7A shows that when I_{to} conductance and inactivation kinetics are comparable to those measured in LV myocytes ($g_{to,si}$ = 0.025 mS/μF, $g_{to,fi}$ = 0.08 mS/μF, τ_{si} = 50 ms), the AP produced a long plateau at high V_m (solid blue curve) with long APDs (> 700ms). In contrast, when I_{to} conductance and inactivation kinetics are comparable to those measured in RV myocytes ($g_{to,si}$ = 0.050 mS/μF, $g_{to,fi}$ =

0.08 mS/μF, τ_{si} = 80 ms), we see an AP waveform similar to that found in experiments, with long APD due to many EADs (Figure 7A solid red curve). When parameters are altered to include the I_{Ks} current to model LMC1 RV and LV, AP traces show much shorter APD without EAD formation in both cell types (blue and red dashed lines in LV and RV, respectively). To further elucidate the role of I_{to} in EAD formation, we distinguish in Figure 7B the contributions of the fast- and slow-inactivating components of I_{to}, $I_{to,fi}$ (FI) and $I_{to,si}$ (SI), respectively. Two main differences of I_{to} properties between the LV and RV can be distinguished. Firstly, the larger peak I_{to} in the RV produces a faster initial repolarization during phase 1 of the AP (i.e. a larger notch). Secondly, the larger amplitude of the slow-inactivating component of I_{to} ($I_{to,si}$) in the RV makes a dominant contribution to the subsequent repolarization during phase 2 of the AP (t<200 msec), thereby bringing the voltage into the window range for reactivation of $I_{Ca,L}$ and promoting EADs. Figure 7C shows that re-activation of $I_{Ca,L}$ coincides with EADs in RV, while in LV repolarization is complete before $I_{Ca,L}$ sufficiently recovers from inactivation to initiate an EAD during late phase 3 of the AP. The faster rate of repolarization during late phase 3 in LV is due to I_{Kr} (Figure 7D), which activates significantly more in LV than RV due to the long AP plateau at high V_m. Figure 7E directly compares I_{Kr} at the same V_m and shows that I_{Kr} contributes twice as much to repolarization in LV than RV in the −20 to +10 mV range relevant to EAD onset.

Figure 7F shows that, with addition of I_{Ks} into the model, EADs become fewer with increasing I_{Ks} conductance and vanish for a normal value of g_{Ks} corresponding to LMC myocytes. Figure 7F also shows the importance of varying I_{to} conductance in absence of I_{Ks}. When I_{to} conductance is small ($g_{to,si}$<0.04 ms/μF), as in LQT1 LV CMs, the high V_m AP plateau prevents EAD formation, despite APD prolongation. For greater I_{to} conductance, as in LQT1 RV CMs, multiple EADs occur (green square on the y axis for g_{Ks} = 0). In this case, I_{to} conductance is large enough for V_m to traverse the critical window for reactivation of $I_{Ca,L}$ before sufficient activation of I_{Kr}, but small enough to avoid complete repolarization, allowing EADs.

To further demonstrate the important role of slow I_{Kr} activation kinetics in EADs formation, we repeated the simulations represented in Figure 7F using a Hodgkin-Huxley (HH) formulation of I_{Kr} with parameters fitted to our voltage-clamp data (Figure S10). The results shown in Figure S10 reproduce the RV and LV AP phenotypes obtained with the multi-state Markov I_{Kr} model (compare Figures 7A–D with Figures S10A–D). Furthermore, in Figures S10E–F, we compare the steady-state activation/inactivation curves and activation-time constant for the new I_{Kr} HH formulation fitted to our voltage-clamp data and the Zeng et al HH I_{Kr} formulation[18] commonly used in rabbit ventricular myocyte ionic models. This comparison underscores the importance of accurate modeling of I_{Kr} activation kinetics to elucidate arrhythmogenic mechanisms in the setting of LQT1 where I_{Ks} is absent.

Discussion

LQT1 is the most common form of long QT syndrome and accounts for almost half of genotyped cases.[2] Pore missense mutations that confer loss of function with dominant negative effect are associated with a more severe form of the disease with a higher frequency

of cardiac events.[19] This study highlights the crucial role of I_{to} in repolarization when I_{Ks} is absent and elucidates the molecular underpinning for the malignant phenotype of LQT1. At the organ level, we found that the heterogeneity of I_{to} underlies pVT initiation by creating APD dispersion and EAD formation that propagates unidirectionally to the RV region to form a reentry. Consistent with those observations, we found that cellular EADs are present in myocytes isolated from RV, but absent from LV myocytes despite much prolonged APD in LV. Computer modeling, combined with detailed voltage-clamp and confocal Ca^{2+} imaging, revealed that heterogeneity in I_{to}, both in terms of amplitude and inactivation kinetics, causes membrane voltage to traverse the window for reactivation of $I_{Ca,L}$ sooner, before I_{Kr} has had sufficient time to activate and prevent the depolarization that underlies EAD formation and pVTs.

EADs formation has been traditionally associated with an instability of V_m dynamics driven by reactivation of $I_{Ca,L}$ during the plateau phase of the AP.[20, 21] While $I_{Ca,L}$ is a necessary depolarizing current to induce EADs, several other membrane currents have been shown experimentally or computationally to modulate EAD formation, including I_{NCX}[14, 22], I_{Ks}[23], and $I_{to.}$[23] The present study highlights heterogeneity in I_{to} amplitude and inactivation kinetics as major factors in the initiation of EADs and reentry in LQT1 rabbits.

The role of I_{to} in the genesis of EADs has also been highlighted in previous experimental and computational studies in isolated rabbit ventricular myocytes exposed to oxidative stress[23, 24] or hypokalemia.[24]. A main finding of those studies is that, even though I_{to} helps repolarization, blocking this current can (counter-intuitively) suppress EADs. This paradoxical effect is linked mechanistically to the fact that Ito can lower the AP plateau voltage into a range where activation of IKs is slowed sufficiently to allow reactivation of ICa,L and induction of EADs.[23, 24] Importantly, I_{to} is also implicated in arrhythmogenesis in Brugada syndrome. By contrast, deletions of I_{to} in several models in mice were not associated with sudden cardiac death.[25] Our results highlight a similar mechanism of Ito in LQT1 rabbits, but with the slow activation of IKr allowing reactivation of ICa,L when the lower AP plateau voltage is reached rapidly.

Two factors may precipitate pVT initiation in LQT1 rabbits: i) APD gradient between RV and LV and ii) EAD formation from the short-APD region. Enhanced APD dispersion has been well recognized as a substrate for reentry in LQTS.[4, 26] However, in order to initiate reentry, the propagating AP must encounter a conduction block. In LQT1, because EADs form in RV where APD is shorter, the propagation of EADs eventually reaches the LV region where APD is longer, causing conduction block and initiation of reentry (Figure 1). Therefore, this study emphasizes the importance of I_{to} heterogeneity, which allows EAD formation in the short-APD region, and forming unidirectional conduction and reentry in LQT1 rabbits.

I_{to} heterogeneity between RV and LV[27, 28], and also epi- to endocardium[13, 29], has been well recognized. In our transgenic rabbit model of LQT1, I_{to} heterogeneity between RV and LV may have greater impact on arrhythmogenesis but in large animals including human, transmural heterogeneity of I_{to} can also have significant impact on EADs and reentry formation due to sufficient transmural dimension to form reentry. Two major transient

outward (I_{to}) currents are likely responsible for this current in large mammals: $I_{to,s}$ (Kv1.4), and $I_{to,f}$ (Kv4.2 and Kv4.3), which differ in their recovery-time constants[12, 30] but both of which have multi-exponential inactivation kinetics[12]. Even though previous work suggests that the main component in rabbits is $I_{to,s}$, our double-pulse voltage-clamp study demonstrated that $I_{to,f}$ in rabbit RV constitutes ~28% of total I_{to} and is the major component that underlies a large I_{to} in RV (Figure 4). Our western blot study demonstrated that I_{to} heterogeneity is associated with KChIP2 expression level (Figure 4E). KChIP2 has been reported to increase trafficking and expression of Kv4.2 and Kv4.3 that underlie $I_{to,f}$.[31] KChIP2 slows I_{to} inactivation kinetics[32], which may partly explain the molecular mechanisms underlying greater I_{to} in RV. However, further studies are needed to clarify the origin of the greater amplitude of the slow-inactivating component of I_{to} ($I_{to,si}$) in RV (Figure 3 and 4) and its potential transmural heterogeneity, which is potentially linked to different phosphorylated states of Kv1.4 and Kv4.2/4.3 channels in RV and LV[12, 30]

Our computer modeling study showed that $I_{to,si}$ plays a crucial role in determining the plateau V_m and initiating EADs (Figure 7 and Figure S12). $I_{to,si}$ recovers to a larger amplitude in rabbit RV than LV at moderately slow heart rate > 600 ms (Figure 4). This may explain why LQT1 rabbits show dramatically more SCDs after bradycardia caused by AV node ablation.[33]

I_{to} heterogeneity is no greater in LQT1 than in LMC (supplemental figure S4). However, this heterogeneity has a greater impact on pVT initiation in LQT1 than in LMC (supplementary Figure S2–3), where I_{Ks} abolishes the arrhythmogenic effect of I_{to} at a cellular level (Figure 7F). Previous computer modeling studies of LQT1 found critical roles of I_{Ks} on APD prolongation[34] and EAD formation under reduced I_{Kr} condition.[35] In particular, the study by O'Hara and Rudy[35] showed that, in addition to isoproterenol, partial block of I_{Kr} was needed to evoke EADs when I_{Ks} kinetics is altered by the Q357R KCNQ1 mutation while in the present study isoproterenol suffices to evoke EADs without block of I_{Kr} in the absence I_{Ks}. Since I_{to} is heterogeneously expressed even in normal myocardium between RV and LV as well as epi- and endocardium,[12, 13, 36] our study suggests that I_{Ks} has an important protective role beyond repolarization reserve by acting as a safety mechanism that counters the arrhythmogenic effect of I_{to} heterogeneity revealed by the present study. Hence, the main consequence of the loss of function of I_{Ks} is to unmask the arrhythmogenic role of I_{to} heterogeneity, which is masked by I_{Ks} in LMC hearts.

Regarding Ca^{2+}-handling proteins, the hyperphosphorylation of RyR was recently shown to play an important role in the genesis of EADs in myocytes isolated from LQT2 transgenic rabbits carrying a loss-of-function mutation of the HERG potassium channel encoding the I_{Kr} channels.[14] Experiments and computational modeling demonstrated that EADs are promoted by aberrant late Ca^{2+} releases by hyperactivity of RyR Ca^{2+} channels. The Ca^{2+}-handling machinery under isoproterenol in LQT1, however, is not markedly different between myocytes forming EADs (RV) vs. myocytes not forming EADs (LV), indicating that EAD formation in RV cannot be ascribed to differences in Ca^{2+} homeostasis in RV vs. LV (Figure 6). However, it is still possible that sustained Ca^{2+} release during AP plateau can influence APDs and further studies are needed for potential roles of Ca^{2+} handling in LQT1.

Our voltage-clamp data from both LMC and LQT1 rabbits demonstrated the existence of both fast and slow components of I_{Kr} activation, with the slow component being dominant for V_m up to 10 mV. Unless V_m is high for a long duration (such as in LQT1 LV CMs), this dominant slow component will prevent I_{Kr} from significantly activating, which is key for EAD formation (supplemental Figure S9 and S10). Since I_{Kr} activation and deactivation kinetics are similar in rabbits and humans,[37] our results suggest that I_{Kr} kinetics is likely to play an important role in LQT1 EAD formation.

Limitations

This study focuses on the role of I_{to} in the initiation of EADs through determining the trajectory of V_m during phase 1 of early repolarization, but did not study the potential effects of sustained I_{to} that may also have contributed to the maintenance of multiple EADs. $I_{to,s}$ is the major component of I_{to} in rabbits, and EADs in different species (including humans) may occur at faster heart rates. In optical mapping, 4-AP may have non-specific action on I_{Kr} and further prolong APD. Chromanol is known to alter I_{to} at higher concentrations, and I_{to} measurements in LMC myocytes may have been underestimated.

Conclusion

Using a transgenic rabbit model of LQT1 and computer modeling, we demonstrated that I_{to} plays a key role in arrhythmogenesis, creating both triggers and an arrhythmogenic substrate for reentry. When I_{Ks} is absent, complex interactions between I_{to}, I_{CaL}, and I_{Kr} transduce the marked heterogeneity of I_{to} properties into a marked heterogeneity of the AP phenotype leading to pVT initiation. This study suggests that I_{to} is a major contributor to LQT-related arrhythmias and that its heterogeneity may underlie regional EAD formation and initiation of pVTs.

Supplementary Material

Refer to Web version on PubMed Central for supplementary material.

Acknowledgments

Sources of Funding: This work was supported by the National Heart, Lung, and Blood Institute at the National Institutes of Health R01HL110791 to G.K., R01HL096669 to B.C, and R01HL121796 to D.T.

References

1. Wang Q, Curran ME, Splawski I, Burn TC, Millholland JM, VanRaay TJ, Shen J, Timothy KW, Vincent GM, de Jager T, Schwartz PJ, Toubin JA, Moss AJ, Atkinson DL, Landes GM, Connors TD, Keating MT. Positional cloning of a novel potassium channel gene: KVLQT1 mutations cause cardiac arrhythmias. Nat Genet. 1996; 12:17–23. [PubMed: 8528244]
2. Splawski I, Shen J, Timothy KW, Lehmann MH, Priori S, Robinson JL, Moss AJ, Schwartz PJ, Towbin JA, Vincent GM, Keating MT. Spectrum of mutations in long-QT syndrome genes. KVLQT1, HERG, SCN5A, KCNE1, and KCNE2. Circulation. 2000; 102:1178–1185. [PubMed: 10973849]
3. Moss AJ, Robinson JL, Gessman L, Gillespie R, Zareba W, Schwartz PJ, Vincent GM, Benhorin J, Heilbron EL, Towbin JA, Priori SG, Napolitano C, Zhang L, Medina A, Andrews ML, Timothy K. Comparison of clinical and genetic variables of cardiac events associated with loud noise versus

swimming among subjects with the long QT syndrome. Am J Cardiol. 1999; 84:876–879. [PubMed: 10532503]

4. Shimizu W, Antzelevitch C. Cellular basis for long QT, transmural dispersion of repolarization, and torsade de pointes in the long QT syndrome. J Electrocardiol. 1999; 32:177–184. [PubMed: 10688323]
5. Volders PG, Stengl M, van Opstal JM, Gerlach U, Spatjens RL, Beekman JD, Sipido KR, Vos MA. Probing the contribution of IKs to canine ventricular repolarization: key role for beta-adrenergic receptor stimulation. Circulation. 2003; 107:2753–2760. [PubMed: 12756150]
6. Takenaka K, Ai T, Shimizu W, Kobori A, Ninomiya T, Otani H, Kubota T, Takaki H, Kamakura S, Horie M. Exercise stress test amplifies genotype-phenotype correlation in the LQT1 and LQT2 forms of the long-QT syndrome. Circulation. 2003; 107:838–844. [PubMed: 12591753]
7. Burashnikov A, Antzelevitch C. Block of I(Ks) does not induce early afterdepolarization activity but promotes beta-adrenergic agonist-induced delayed afterdepolarization activity. J Cardiovasc Electrophysiol. 2000; 11:458–465. [PubMed: 10809500]
8. Virag L, Jost N, Papp R, Koncz I, Kristof A, Kohajda Z, Harmati G, Carbonell-Pascual B, Ferrero JM Jr, Gy Papp J, Nanasi PP, Varro A. Analysis of the contribution of Ito to repolarization in canine ventricular myocardium. Br J Pharmacol. 2011
9. Brunner M, Peng X, Liu GX, Ren XQ, Ziv O, Choi BR, Mathur R, Hajjiri M, Odening KE, Steinberg E, Folco EJ, Pringa E, Centracchio J, Macharzina RR, Donahay T, Schofield L, Rana N, Kirk M, Mitchell GF, Poppas A, Zehender M, Koren G. Mechanisms of cardiac arrhythmias and sudden death in transgenic rabbits with long QT syndrome. J Clin Invest. 2008; 118:2246–2259. [PubMed: 18464931]
10. Kim TY, Kunitomo Y, Pfeiffer Z, Patel D, Hwang J, Harrison K, Patel B, Jeng P, Ziv O, Lu Y, Peng X, Qu Z, Koren G, Choi BR. Complex excitation dynamics underlie polymorphic ventricular tachycardia in a transgenic rabbit model of long QT syndrome type 1. Heart Rhythm. 2015; 12:220–228. [PubMed: 25285647]
11. Liu GX, Choi BR, Ziv O, Li W, de Lange E, Qu Z, Koren G. Differential conditions for early after-depolarizations and triggered activity in cardiomyocytes derived from transgenic LQT1 and LQT2 rabbits. J Physiol. 2012; 590:1171–1180. [PubMed: 22183728]
12. Patel SP, Campbell DL. Transient outward potassium current, 'Ito', phenotypes in the mammalian left ventricle: underlying molecular, cellular and biophysical mechanisms. J Physiol. 2005; 569:7–39. [PubMed: 15831535]
13. Brahmajothi MV, Campbell DL, Rasmusson RL, Morales MJ, Trimmer JS, Nerbonne JM, Strauss HC. Distinct transient outward potassium current (Ito) phenotypes and distribution of fast-inactivating potassium channel alpha subunits in ferret left ventricular myocytes. J Gen Physiol. 1999; 113:581–600. [PubMed: 10102938]
14. Terentyev D, Rees CM, Li W, Cooper LL, Jindal HK, Peng X, Lu Y, Terentyeva R, Odening KE, Daley J, Bist K, Choi BR, Karma A, Koren G. Hyperphosphorylation of RyRs underlies triggered activity in transgenic rabbit model of LQT2 syndrome. Circ Res. 2014; 115:919–928. [PubMed: 25249569]
15. Mahajan A, Shiferaw Y, Sato D, Baher A, Olcese R, Xie LH, Yang MJ, Chen PS, Restrepo JG, Karma A, Garfinkel A, Qu Z, Weiss JN. A rabbit ventricular action potential model replicating cardiac dynamics at rapid heart rates. Biophys J. 2008; 94:392–410. [PubMed: 18160660]
16. Mazhari R, Greenstein JL, Winslow RL, Marban E, Nuss HB. Molecular interactions between two long-QT syndrome gene products, HERG and KCNE2, rationalized by in vitro and in silico analysis. Circ Res. 2001; 89:33–38. [PubMed: 11440975]
17. Nemec J, Kim JJ, Salama G. The link between abnormal calcium handling and electrical instability in acquired long QT syndrome - Does calcium precipitate arrhythmic storms? Prog Biophys Mol Biol. 2016; 120:210–221. [PubMed: 26631594]
18. Zeng J, Laurita KR, Rosenbaum DS, Rudy Y. Two components of the delayed rectifier K+ current in ventricular myocytes of the guinea pig type. Theoretical formulation and their role in repolarization. Circ Res. 1995; 77:140–152. [PubMed: 7788872]
19. Moss AJ, Shimizu W, Wilde AA, Towbin JA, Zareba W, Robinson JL, Qi M, Vincent GM, Ackerman MJ, Kaufman ES, Hofman N, Seth R, Kamakura S, Miyamoto Y, Goldenberg I,

Andrews ML, McNitt S. Clinical aspects of type-1 long-QT syndrome by location, coding type, and biophysical function of mutations involving the KCNQ1 gene. Circulation. 2007; 115:2481–2489. [PubMed: 17470695]

20. Qu Z, Xie LH, Olcese R, Karagueuzian HS, Chen PS, Garfinkel A, Weiss JN. Early afterdepolarizations in cardiac myocytes: beyond reduced repolarization reserve. Cardiovasc Res. 2013; 99:6–15. [PubMed: 23619423]
21. January CT, Riddle JM. Early afterdepolarizations: mechanism of induction and block. A role for L-type Ca2+ current. Circ Res. 1989; 64:977–990. [PubMed: 2468430]
22. Xie Y, Grandi E, Puglisi JL, Sato D, Bers DM. beta-adrenergic stimulation activates early afterdepolarizations transiently via kinetic mismatch of PKA targets. J Mol Cell Cardiol. 2013; 58:153–161. [PubMed: 23481579]
23. Zhao Z, Xie Y, Wen H, Xiao D, Allen C, Fefelova N, Dun W, Boyden PA, Qu Z, Xie LH. Role of the transient outward potassium current in the genesis of early afterdepolarizations in cardiac cells. Cardiovasc Res. 2012; 95:308–316. [PubMed: 22660482]
24. Nguyen TP, Singh N, Xie Y, Qu Z, Weiss JN. Repolarization reserve evolves dynamically during the cardiac action potential: effects of transient outward currents on early afterdepolarizations. Circ Arrhythm Electrophysiol. 2015; 8:694–702. [PubMed: 25772542]
25. Brunner M, Guo W, Mitchell GF, Buckett PD, Nerbonne JM, Koren G. Characterization of mice with a combined suppression of I(to) and I(K,slow). Am J Physiol Heart Circ Physiol. 2001; 281:H1201–1209. [PubMed: 11514288]
26. Napolitano C, Priori SG, Schwartz PJ. Significance of QT dispersion in the long QT syndrome. Prog Cardiovasc Dis. 2000; 42:345–350. [PubMed: 10768312]
27. Di Diego JM, Sun ZQ, Antzelevitch C. I(to) and action potential notch are smaller in left vs. right canine ventricular epicardium. Am J Physiol. 1996; 271:H548–561. [PubMed: 8770096]
28. Volders PG, Sipido KR, Carmeliet E, Spatjens RL, Wellens HJ, Vos MA. Repolarizing K+ currents ITO1 and IKs are larger in right than left canine ventricular midmyocardium. Circulation. 1999; 99:206–210. [PubMed: 9892584]
29. Nabauer M, Beuckelmann DJ, Uberfuhr P, Steinbeck G. Regional differences in current density and rate-dependent properties of the transient outward current in subepicardial and subendocardial myocytes of human left ventricle. Circulation. 1996; 93:168–177. [PubMed: 8616924]
30. Guo W, Li H, London B, Nerbonne JM. Functional consequences of elimination of i(to,f) and i(to,s): early afterdepolarizations, atrioventricular block, and ventricular arrhythmias in mice lacking Kv1. 4 and expressing a dominant-negative Kv4 alpha subunit. Circ Res. 2000; 87:73–79. [PubMed: 10884375]
31. Rosati B, Grau F, Rodriguez S, Li H, Nerbonne JM, McKinnon D. Concordant expression of KChIP2 mRNA, protein and transient outward current throughout the canine ventricle. J Physiol. 2003; 548:815–822. [PubMed: 12598586]
32. Patel SP, Parai R, Parai R, Campbell DL. Regulation of Kv4. 3 voltage-dependent gating kinetics by KChIP2 isoforms. J Physiol. 2004; 557:19–41. [PubMed: 14724186]
33. Gravelin L, Ziv O, Liu G, Hartmann K, Patel D, Schofield L, Chaves L, Shearer M, Koren G, Choi B. Heart Rhythm. Denver, Colorado: 2012. Transgenic LQT1 Animal Model Reveals EADs and Multifocal Activity as Mechanism for polymorphic Ventricular Tachycardia (pVT); PO3–104.
34. Hoefen R, Reumann M, Goldenberg I, Moss AJ, JOU, Gu Y, McNitt S, Zareba W, Jons C, Kanters JK, Platonov PG, Shimizu W, Wilde AA, Rice JJ, Lopes CM. In silico cardiac risk assessment in patients with long QT syndrome: type 1: clinical predictability of cardiac models. J Am Coll Cardiol. 2012; 60:2182–2191. [PubMed: 23153844]
35. O'Hara T, Rudy Y. Arrhythmia formation in subclinical ("silent") long QT syndrome requires multiple insults: quantitative mechanistic study using the KCNQ1 mutation Q357R as example. Heart Rhythm. 2012; 9:275–282. [PubMed: 21952006]
36. Antzelevitch C, Fish J. Electrical heterogeneity within the ventricular wall. Basic Res Cardiol. 2001; 96:517–527. [PubMed: 11770069]
37. Cheng JH, Kodama I. Two components of delayed rectifier K+ current in heart: molecular basis, functional diversity, and contribution to repolarization. Acta Pharmacol Sin. 2004; 25:137–145. [PubMed: 14769199]

WHAT IS KNOWN?

- Long QT syndrome type 1 (LQT1), an inherited disease caused by loss-of-function mutations in KCNQ1, is associated with sudden cardiac arrest triggered by early afterdepolarizations (EADs).
- EADs have been traditionally associated with an instability of V_m dynamics driven by reactivation of the L-type Ca^{2+} current ($I_{Ca,L}$) during the plateau phase of the action potential that initiates polymorphic VT (pVT).

WHAT THE STUDY ADDS?

- It uses a transgenic rabbit model of LQT1 to shed light on the mechanisms of EADs formation and pVT initiation at the cellular and organ scales.
- It finds that the transient outward K^+ current (I_{to}) is both significantly larger and inactivates more slowly in the right ventricle (RV) than the left ventricle (LV), and links mechanistically this regional variation of I_{to} properties to the observed regional variation of EADs frequency, abundant in the RV but absent in the LV.
- It shows that larger I_{to} in the RV causes V_m to traverse the critical window range for reactivation of $I_{Ca,L}$ earlier during the AP plateau before sufficient activation of I_{Kr} promoting EADs formation in the short-APD region. These EADs propagate uni-directionally to form reentry and polymorphic ventricular tachycardia (VT).

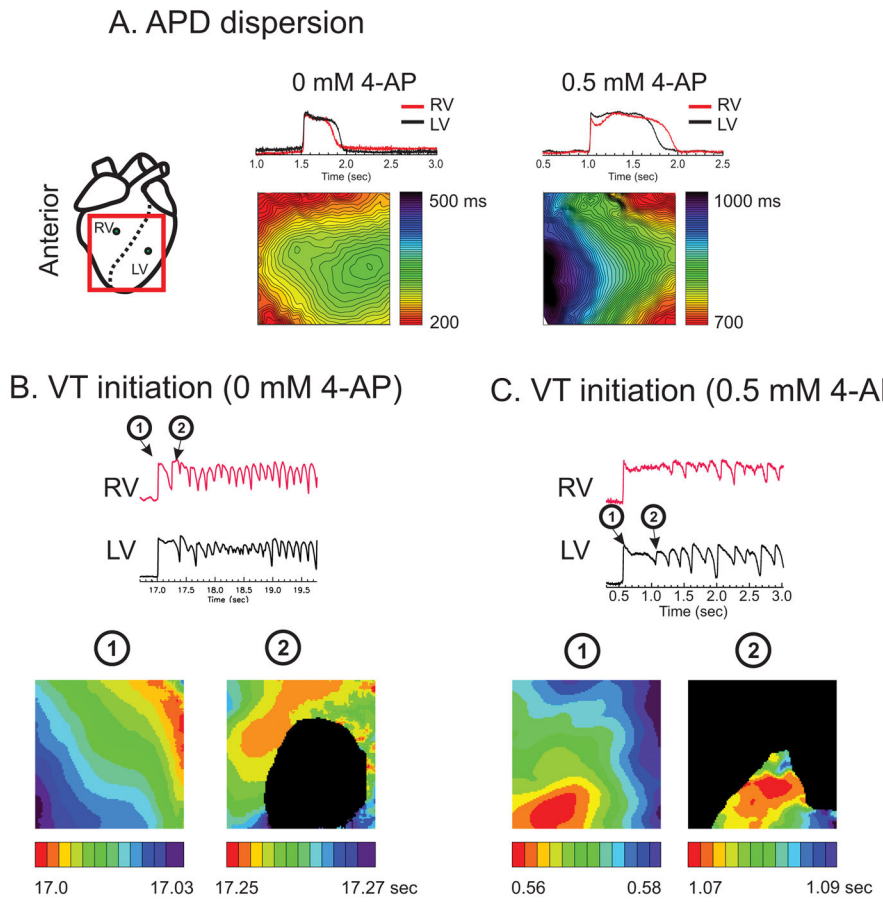

Figure 1.

A) APD maps under 4-AP. APD is longer in LV under normal conditions in LQT1 but 4-AP prolonged APDs (135% increase from 312 ± 63 to 729 ± 143 ms at 0.5 Hz) and flipped the APD gradient, resulting in longer APD in RV (n=4/5 hearts, Fisher exact test $p < 0.05$). B) RV initiation of pVT in LQT1 hearts (RV initiation 83% of pVT events, n=5/5 hearts, $p < 0.05$[10]). C) LV initiation of pVT in LV after 0.5 mM 4-AP (n=4/5 hearts, Fisher exact test $p < 0.05$). The black area indicates failed activation due to conduction block (Movies of activation are provided as supplemental material movie S1 and S2).

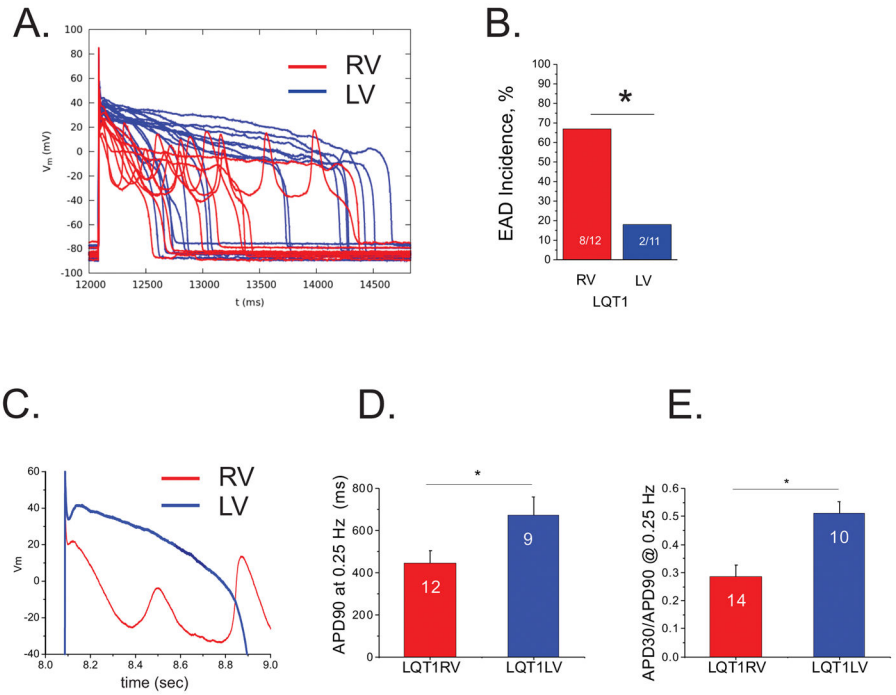

Figure 2.

Frequent EADs despite shorter APD in RV myocytes. A) Representative V_m traces recorded from RV (red, n=12 cells) and LV (blue, n=11 cells) myocytes in 50 nM isoproterenol. B) EAD incidence. EADs were frequently in LQT1 RV myocytes (67% in RV vs. 0.18 % LV myocytes, Fisher's exact test; $p < 0.05$). C) Detail traces of initial action potential repolarization phase in expanded time scale. Note that the initial rapid repolarization in RV cells is associated with EAD formation. D & E) APD_{90} and APD_{30}/APD_{90}. APD_{90} from LV cells showed prolonged APD despite lack of EADs. APD_{30}/APD_{90} indicates that RV cells have lower V_m during plateau phase, showing an association between rapid initial repolarization phase and EAD formation, suggesting a potential role of I_{to} in EAD formation (ANOVA, $p < 0.05$).

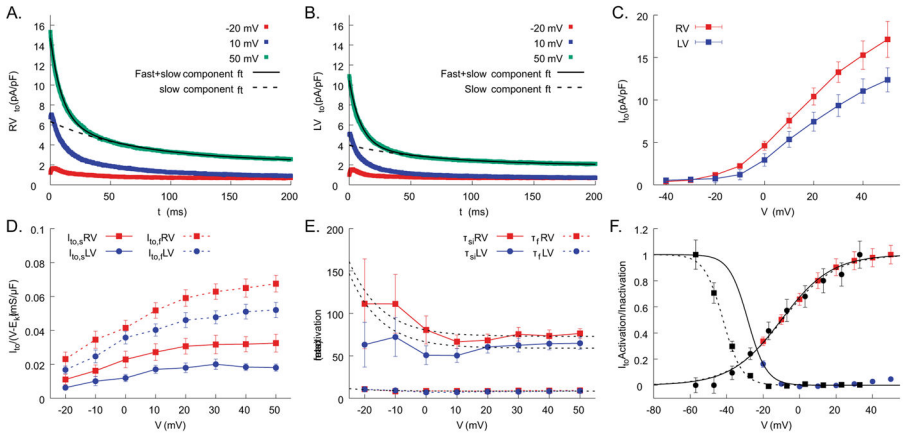

Figure 3.

Amplitude and inactivation kinetics of I_{to} are markedly different between RV and LV cells. Sample voltage clamp traces for I_{to} from RV (A) and LV cells (B). The inactivation kinetics of I_{to} showed two-exponential decays, fast-inactivation component (fi) and slow-inactivation component (si), see methods for detail. C) The total amplitude of I_{to} is 28% larger in RV than LV (17.1 ± 2.1 pA/pF in RV vs. 12.4 ± 1.4 pA/pF in LV at 50 mV, ANOVA $p<0.05$, n=16 and 15 cells for RV and LV from n=5 hearts). D) $I_{to,fi}$ and $I_{to,si}$ from RV (n=16) and LV cells (n=15 from n=5 hearts). Both fast and slow components are greater in RV. E) The fast-inactivation time constants (τ_{fi}) are the same in RV and LV cells, whereas the slow-inactivation time constant (τ_{si}) is longer in RV (see supplemental Table S1). F) mean activation and inactivation curves of $I_{to,total}$ from LQT1 (solid lines) and LMC (dotted lines) myocytes. After normalized to the maximum value, the data were fitted to the Boltzman function and used for computer modeling.

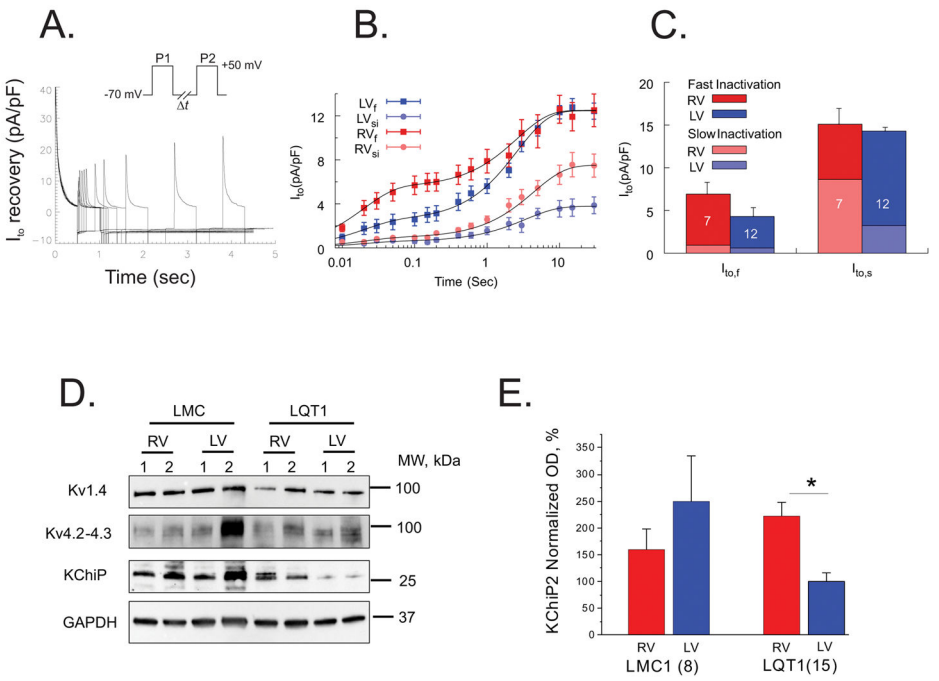

Figure 4.

I_{to} recovery from inactivation. A) The recovery kinetics was tested by a double-pulse protocol with interpulse time varying from 50 ms to 15 sec (n=12 RV and 7 LV cells from n=3 hearts). B) The amplitudes of the slow and fast inactivating components of I_{to} ($I_{to,si}$ and I $I_{to,fi}$) as a function of inter-pulse interval were determined by fitting the time course of I_{to} decay during the second pulse to a double exponential function. The x-axis of inter-pulse intervals is in a logarithmic scale. C) The amplitudes of $I_{to,fi}$ and $I_{to,si}$ from RV and LV. Fast and slow-inactivating components ($I_{to,fi}$ and $I_{to,si}$) of each $I_{to,f}$ and $I_{to,s}$ were calculated as described in Methods and represented as a stacked column plot. D) Western blots of Kv4.2, Kv1.4, and KChIP2 from LQT1 hearts. E). The accessory unit of I_{to}, KChIP2, known to affect inactivation and recovery kinetics, was twofold higher in RV (ANOVA, $p < 0.05$). The currents were measured under 50 nM isoproterenol. Additional Kv4.2 and Kv1.4 gel analyses are provided in the supplemental material.

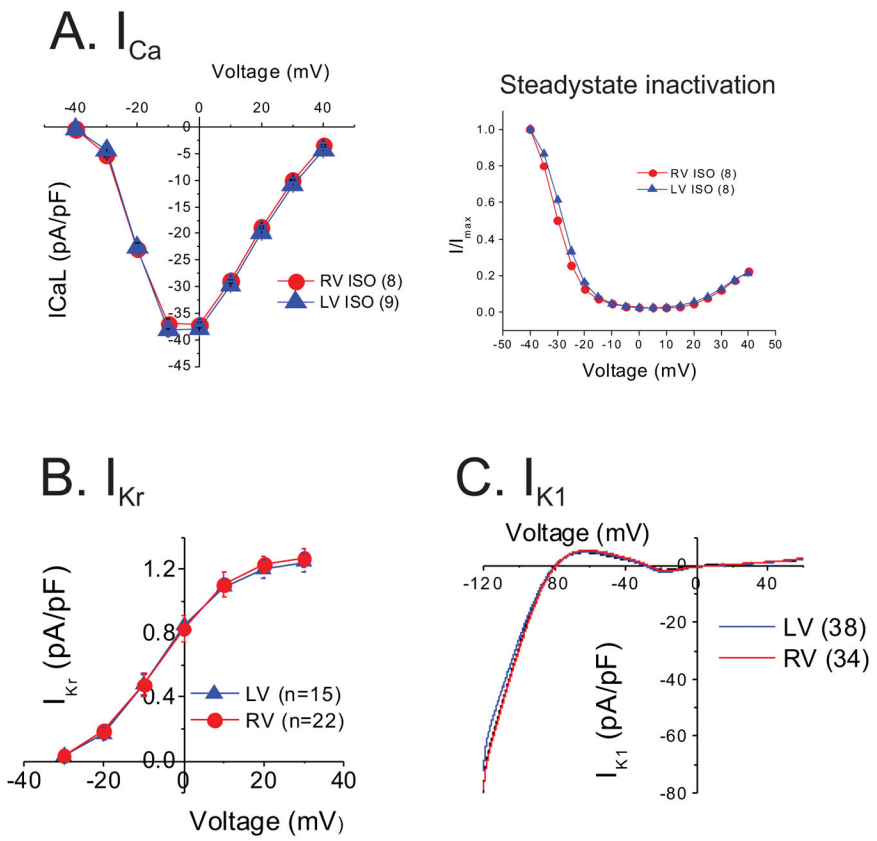

Figure 5.

$I_{Ca,}$ (A), I_{Kr} (B), and I_{K1} (C) did not differ between RV and LV cells. All currents were measured under 50 nM isoproterenol.

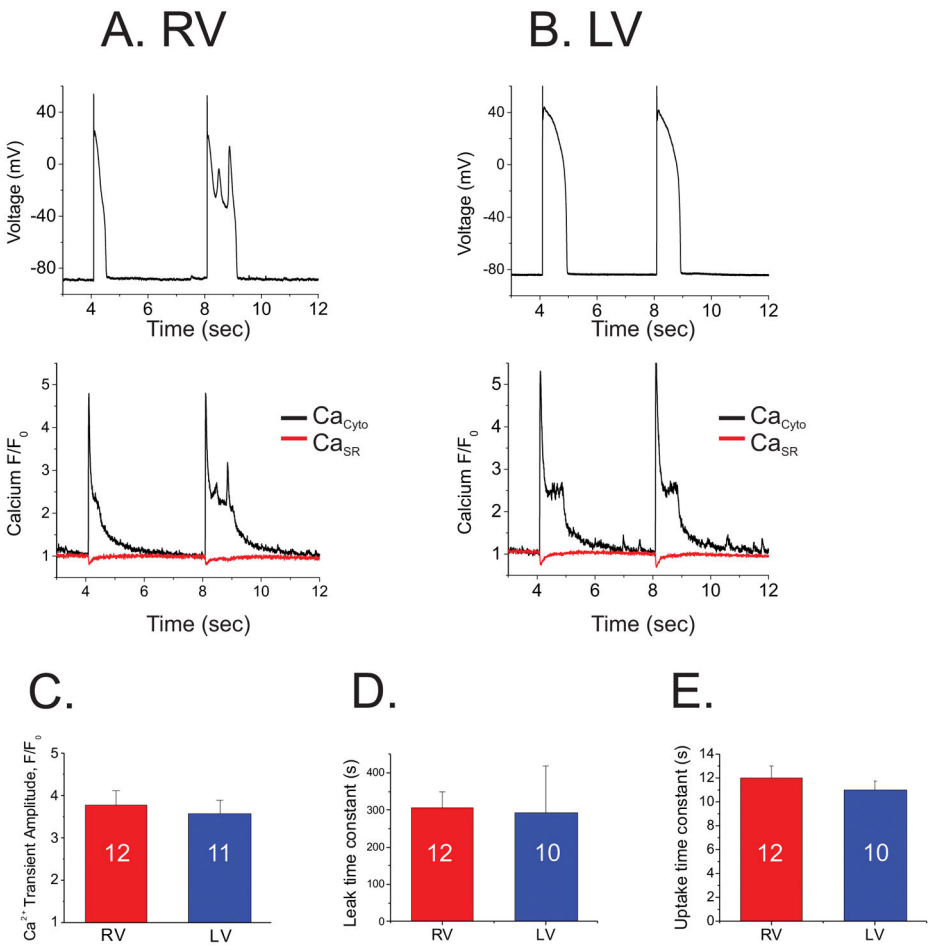

Figure 6.

Ca^{2+} handling is not responsible for preferential EAD formation from RV cells. A & B) Simultaneous recordings of V_m, Ca^{2+} transients (Ca_{Cyto}), and SR Ca^{2+} contents (Ca_{SR}) from single RV and LV cells. Note that higher Ca^{2+} level during action potential plateau in LV did not trigger EADs. C) Amplitudes of Ca^{2+} transients. D) Ca^{2+} leak from RyR. E) Ca^{2+} uptake. Ca^{2+} handling was not markedly different between RV and LV cells.

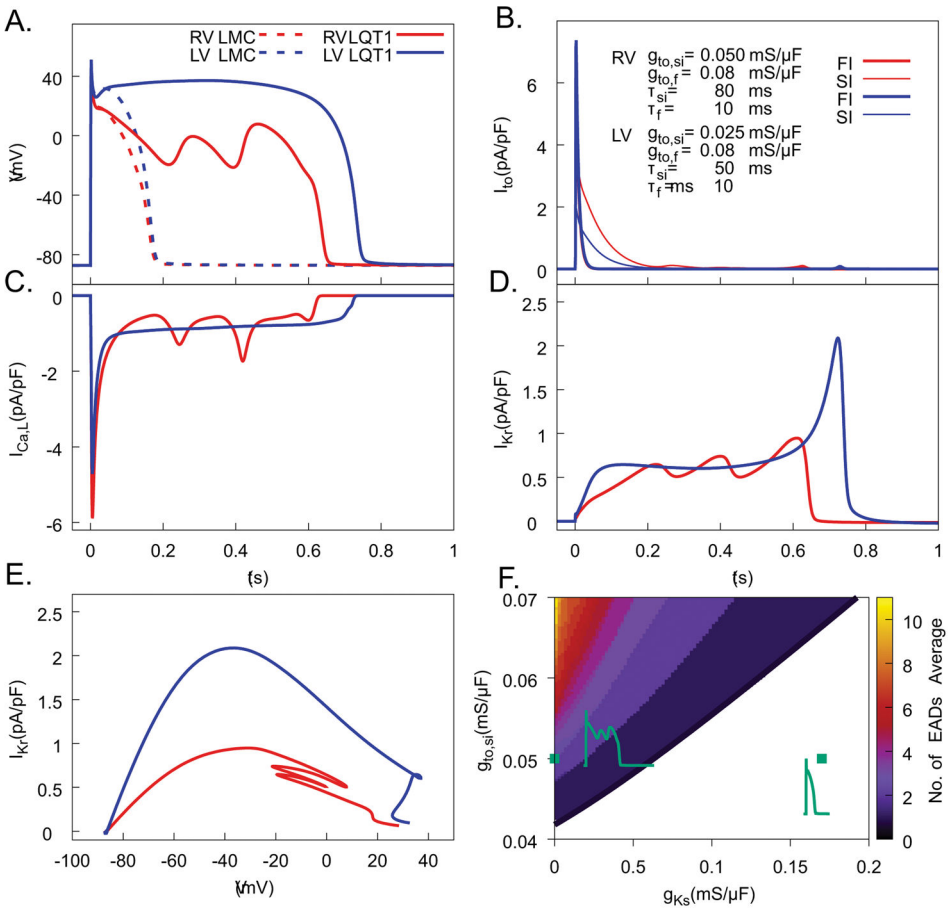

Figure 7.

Computer modeling study of EADs reproduces I_{to}-dependent EADs in LQT1 myocytes under isoproterenol stimulation. A) Computed V_m traces for different I_{to} model parameters fitted to voltage-clamp measurements of I_{to} in RV and LV cells of LQT1 and LMC rabbits. Only RV (red) from LQT1 demonstrated EADs. B) I_{to} traces broken into fast-inactivating component (red in RV, dark blue in LV) and slowly inactivating component (orange in RV, light blue in LV) for action potentials in panel A. C) I_{CaL} from RV (red) and LV (blue) during action potentials in panel A. D) I_{Kr} during action potentials in panel A. E) Dynamic I–V curves showing I_{Kr} during repolarization as a function of V_m. Note that in the range of V_m oscillations during EADs, I_{Kr} from RV (red) is markedly lower than LV (blue). F) EAD formation in the parameter space of $I_{to,si}$ conductance ($g_{to,si}$, Y axis) vs. I_{Ks} conductance (g_{Ks}, X axis) with and other parameters $g_{to,fi}$ = 0.074 mS/μF, τ_{si} = 69 ms, and τ_{fi} = 8.5 ms. Representative AP traces within each region are shown, with parameters indicated by green diamonds. The right-most green diamond corresponds to parameters representative of LMC cells.